UDC 535.34.546.26

EXTENDED ANALYSIS OF THE UV–VIS ABSORPTION SPECTRUM OF GRAPHENE OXIDE. URBACH ENERGY, TAUC MODEL AMBIGUITY AND sp^2 DOMAIN SIZE

Daminov Rakhimjon Shokir ugli,
Nanotechnology Development Center,
National University of Uzbekistan named after
Mirzo Ulugbek, Tashkent, Uzbekistan
daminov_r@nuu.uz
Ochilov Odil,
Nanotechnology Development Center,
National University of Uzbekistan named after
Mirzo Ulugbek, Tashkent, Uzbekistan
ochilovodil@mail.ru
Malikov Komiljon Kholmuratovich,
Nanotechnology Development Center,
National University of Uzbekistan named after
Mirzo Ulugbek, Tashkent, Uzbekistan
komiljonmalikov1995@gmail.com
Yoldoshev Ozodbek Yoldosh ugli
Nanotechnology Development Center,
National University of Uzbekistan named after
Mirzo Ulugbek, Tashkent, Uzbekistan
ozodbekyoldoshev997@gmail.com
Qambarova Mukhayyo Sodikjon kizi
Nanotechnology Development Center,
National University of Uzbekistan named after
Mirzo Ulugbek, Tashkent, Uzbekistan
muhayyoqambarova1@gmail.com
Ne'matova Zumrad Zayniddin kizi
National University of Uzbekistan named
after Mirzo Ulugbek, Tashkent, Uzbekistan
toxirovazumrad@gmail.com

Abstract. *The ultraviolet–visible absorption spectra of graphene oxide synthesized by the Hummers method are analysed, yielding optical parameters not published previously. The Urbach energy is determined for the first time and equals 0.91 ± 0.01 eV, the exponential region spans 2.00–3.45 eV and is concentration-independent. A model comparison rules out a light-scattering artefact. The steepness parameter σ = kT/EU equals 0.028. Three methods of locating the n→π* shoulder differ by up to 20 nm. The sp^2 domain size is evaluated independently from optical and Raman data. The values obtained are proposed as baseline parameters for GO/Fe_3O_4 magneto-optical systems.*

Key words: *graphene oxide, Urbach energy, optical band gap, Tauc method, derivative spectroscopy, n→π* transition, sp^2 domain, disorder, magneto-optics, Hummers method.*

GRAFEN OKSIDINING UV-VIS YUTILISH SPEKTRINI KENGAYTIRILGAN TAHLILI. URBACH ENERGIYASI, TAUC MODELI NOANIQLIGI VA sp^2 DOMEN O'LCHAMI

Annotatsiya. *Maqolada Hummers usulida sintez qilingan grafen oksidining ultrabinafsha-ko'rinuvchi yutilish spektrlari kengaytirilgan tahlil qilinib, ilgari e'lon qilinmagan optik parametrlar aniqlandi. Urbach energiyasi birinchi marta hisoblanib, u 0,91 ± 0,01 eV ni tashkil etdi, eksponensial soha 2,00–3,45 eV kenglikda saqlanadi va natija konsentratsiyaga bog'liq emas. Model taqqoslash yo'li bilan kuzatilgan signal cheti yorug'lik tarqalishi artefakti emasligi ko'rsatildi. Tikkalik parametri σ = kT/EU 0,028 ga teng bo'ldi. n→π* yelkasining holati uchta usulda baholanib, ular orasidagi tafovut 20 nm ga yetishi aniqlandi. sp^2 domen o'lchami optik va Raman ma'lumotlaridan mustaqil baholandi. Olingan qiymatlar GO/Fe_3O_4 magnitooptik tizimlari uchun bazaviy parametrlar sifatida taklif etiladi.*

Kalit so‘zlar: *grafen oksidi, Urbach energiyasi, optik zona kengligi, Tauc usuli, hosila spektroskopiyasi, n→π* o‘tish, sp² domen, tartibsizlik, magnitooptika, Hummers usuli.*

РАСШИРЕННЫЙ АНАЛИЗ СПЕКТРА УФ-ВИДИМОГО ПОГЛОЩЕНИЯ ОКСИДА ГРАФЕНА. ЭНЕРГИЯ УРБАХА, НЕОДНОЗНАЧНОСТЬ МОДЕЛИ ТАУКА И РАЗМЕР sp^2-ДОМЕНОВ

Аннотация. *В статье представлен расширенный анализ спектров ультрафиолетового и видимого поглощения оксида графена, синтезированного методом Хаммерса, в результате которого определены ранее не публиковавшиеся оптические параметры. Впервые рассчитана энергия Урбаха, составившая 0,91 ± 0,01 эВ, экспоненциальная область сохраняется в интервале 2,00–3,45 эВ, а результат не зависит от концентрации. Сравнением моделей показано, что наблюдаемый хвост не является артефактом светорассеяния. Параметр крутизны σ = kT/EU составил 0,028. Положение плеча n→π* оценено тремя методами, расхождение между которыми достигает 20 нм. Размер sp²-доменов независимо оценён по оптическим и рамановским данным. Полученные значения предлагаются как базовые параметры для магнитооптических систем GO/Fe_3O_4.*

Ключевые слова: *оксид графена, энергия Урбаха, оптическая ширина запрещённой зоны, метод Таука, производная спектроскопия, переход n→π*, sp²-домен, разупорядочение, магнитооптика, метод Хаммерса.*

Introduction. Graphene oxide (GO) is a two-dimensional material obtained by the chemical oxidation of graphite, in which sp^2- and sp^3-hybridized carbon regions coexist. Its electronic structure is governed precisely by the ratio of these two regions, and for this reason the accurate measurement of the optical characteristics is of primary importance when GO is applied in optoelectronics, sensing and energy storage devices [1, 2].

UV–Vis spectroscopy is one of the most widely used techniques for characterizing GO, and two indicators are normally extracted from it. the maximum near 230 nm assigned to the π→π* transition of aromatic C=C bonds, and the shoulder near 300 nm assigned to the n→π* transition of the carbonyl group [3, 4]. A third indicator, the optical band gap E_g obtained from the Tauc equation, is also widely reported [5, 6].

However, a considerable spread is observed in the literature for each of these indicators. values of 290–305 nm are quoted for the n→π* shoulder and 3.2–3.9 eV for the optical band gap [3, 4, 7]. Part of this spread does arise from genuine differences in the degree of oxidation between samples. The other part depends on the choice of the data-processing method, yet this second source is almost never quantified.

Furthermore, the Urbach energy E_U, which is a standard descriptor for disordered semiconductors, is only rarely reported for GO [8]. This quantity nevertheless characterizes the width of the distribution of localized states at the band edge and constitutes a direct quantitative measure of the structural disorder introduced by sp^3 defects.

The aim of the present work is, using a single well-characterized GO sample, (i) to determine the Urbach energy, (ii) to locate the n→π* shoulder by three independent methods and thereby quantify the method-dependent spread, (iii) to expose the ambiguity in the transition type within the Tauc model, and (iv) to evaluate the sp² domain size independently from optical and Raman data.

The GO sample synthesized and characterized by Raman, UV–Vis and SEM–EDS in [9] was taken as the object of investigation. The present paper re-processes the absorption spectra of that sample, all the analytical procedures and results reported below were not published in [9].

Object of investigation and methods applied.

Sample. GO was synthesized by the Hummers method [9]. A mixture of 1 g of natural graphite and 0.5 g of $NaNO_3$ was stirred in 75 mL of 98% H_2SO_4 in an ice bath (T < 5 °C) for 30 min, 4 g of $KMnO_4$ was added in small portions over 6 h (T ≤ 20 °C), the reaction was quenched with distilled water and 32% H_2O_2, the precipitate was washed with 1 M HCl and distilled water until pH 6–7 (8000 rpm) and dried at 50 °C for 24 h.

Measurement. UV–Vis absorption spectra were recorded on a Shimadzu UV-1900i spectrophotometer in a quartz cuvette (l = 1 cm) over the 200–600 nm range with a 0.5 nm step at concentrations of 0.01, 0.08 and 0.12 mg·mL^{-1}.

Analysis. The absorption coefficient was calculated as $\alpha = 2.303A/l$. In all the analyses below it is not the absolute value of α but its variation with photon energy that matters, so the results are independent of the proportionality factor.

The Urbach energy was obtained from the relation $\alpha = \alpha_0 \exp(h\nu/E_U)$ as the reciprocal of the slope of the linear region of the ln α versus $h\nu$ dependence [8]. The optical band gap was evaluated from the Tauc equation $(\alpha h\nu)^n = B(h\nu - E_g)$ for $n = 2$ (direct allowed transition) and $n = 1/2$ (indirect transition) [10]. The linear regions were not selected by hand but automatically. the widest window satisfying the condition $R^2 > 0.999$ was searched for. This approach removes the subjectivity involved in choosing the limits of the linear region.

Derivative spectra were computed with a Savitzky–Golay filter (third-order polynomial, window width 11–51 points), and the dependence of the result on the window width was checked separately. The Gaussian deconvolution was performed over the 3.0–6.15 eV range as the sum of two Gaussian components and a background, three different background models — exponential, power-law λ^{-n} and linear — were tested independently.

The size of the sp^2 clusters was estimated from the optical data using the Robertson–O'Reilly cluster model $E_g \approx 2|\beta|/\sqrt{N}$ ($|\beta| = 2.9$ eV, where N is the number of fused aromatic rings) [11], and from the Raman data using the Ferrari–Robertson relation $I_D/I_G = C'(\lambda)L_a^2$ ($C' \approx 0.0055$ Å^{-2}) [12]. All computations were carried out in Python 3 (NumPy, SciPy).

Results obtained and their analysis.

1. Absorption spectrum and the Beer–Lambert law. In the smoothed spectra the π→π* maximum was recorded at 230.5 nm for all three concentrations. The absorbance at 230.5 nm is linear in concentration ($R^2 = 0.9997$) with an intercept of 0.004, that is, effectively zero. From the slope the mass absorption coefficient $\varepsilon_{230} = 7.9$ mL·mg^{-1}·cm^{-1} was determined. This quantity is of practical value for the spectrophotometric control of the concentration of GO dispersions.

2. Dependence of the n→π* shoulder position on the method of estimation. The position of the shoulder was determined by three independent methods (Figure 1). The extremum of the first derivative gave 292.5–294.5 nm, the minimum of the second derivative 304–305 nm, and the Gaussian deconvolution 312.8–312.9 nm.

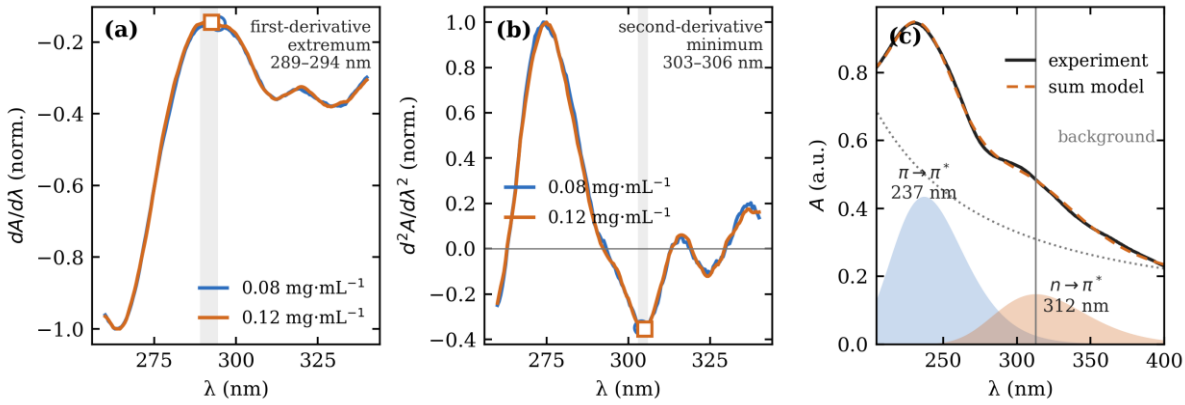


Figure 1. Location of the n→π* shoulder by three methods. (a) first derivative, (b) second derivative, (c) deconvolution into two Gaussian components and an exponential background (0.12 mg·mL^{-1}). The grey bands mark the range of values obtained for the two concentrations.

Each method is highly reproducible within itself. the difference between the two concentrations did not exceed 2 nm, and in the deconvolution the result remained within 311.6–312.9 nm even when the background model was changed three times. Nevertheless, the difference between the methods reached 20 nm, or 0.25 eV in energy units (Table 1).

Table 1. Dependence of the n→π* shoulder position on the method of estimation

Method of estimation	0.08 mg·mL⁻¹	0.12 mg·mL⁻¹	Energy, eV
First-derivative extremum	294.5 nm	292.5 nm	4.21–4.24
Second-derivative minimum	304.0 nm	305.0 nm	4.07–4.08
Gaussian deconvolution	312.9 nm	312.8 nm	3.96
Literature values [3, 4]	300–303 nm	—	4.09–4.13

The reason for the discrepancy is that the shoulder is located on the steeply falling wing of the π→π* band. The extremum of the first derivative merges with the slope of the background and therefore yields a systematically blue-shifted value. The minimum of the second derivative is insensitive to the linear

component of the background, whereas the deconvolution models the background explicitly but relies on an assumption about the line shape.

It follows that a significant part of the 290–305 nm spread observed in the literature originates not from genuine differences between samples but from the choice of the processing method. For this reason the method of determination must be stated whenever the position of the n→π* shoulder is reported, otherwise the results of different studies are not comparable.

3. Ambiguity of the transition type in the Tauc analysis. The direct allowed transition model (n = 2) gave E_g = 3.36 eV in the 3.70–4.15 eV window (R^2 = 0.9992). The indirect transition model (n = 1/2), however, gave E_g = 1.87 eV with practically the same quality of fit (R^2 = 0.9992) in the 3.45–4.05 eV window (Figure 2).

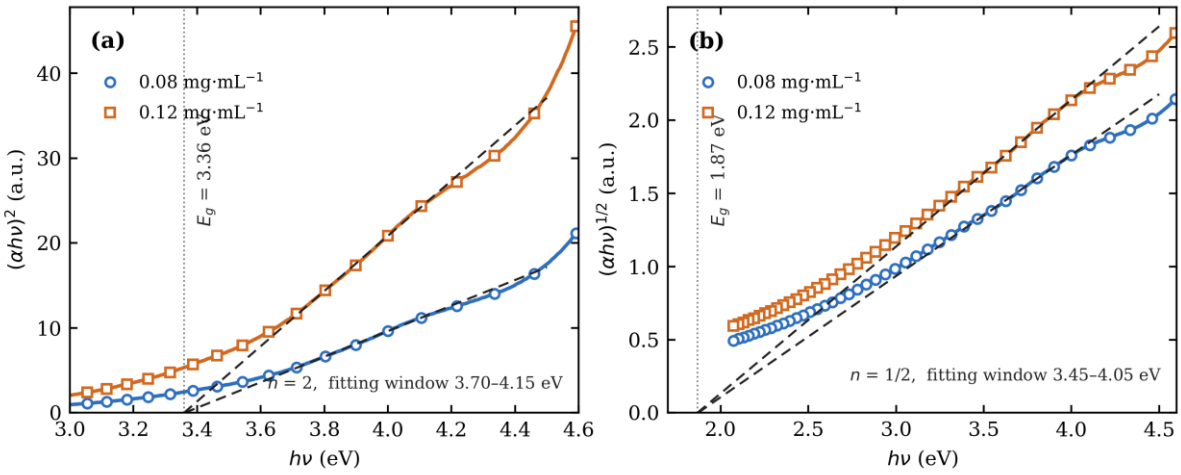


Figure 2. Tauc plots. (a) direct allowed transition, n = 2, (b) indirect transition, n = 1/2. The dashed lines are the extrapolations of the linear region to the energy axis

The fact that both models yield the same coefficient of determination shows that the linearity of a Tauc plot is not evidence confirming the transition type. For GO the value n = 2 is usually adopted in the literature and justified by the allowed character of the π→π* transition [5, 6], but this choice follows from an external physical argument rather than from the plot itself. Consequently, the chosen value of n and the fitting window must always be stated when an E_g value is reported.

4. Urbach energy and structural disorder. The ln α versus $h\nu$ dependence proved to be linear with high accuracy over the 2.00–3.45 eV range, that is, over a region 1.45 eV wide (R^2 = 0.9994, Figure 3a). This yields E_U = 0.919 eV (0.08 mg·mL^{-1}) and 0.904 eV (0.12 mg·mL^{-1}), with a mean value of 0.91 ± 0.01 eV. The difference between the two concentrations did not exceed 1.6%, which confirms that E_U is an intrinsic property of the material and not concentration-dependent. In a narrow range close to the band edge (2.80–3.40 eV) E_U = 0.96–0.98 eV, so the result depends only weakly on the width of the chosen window.

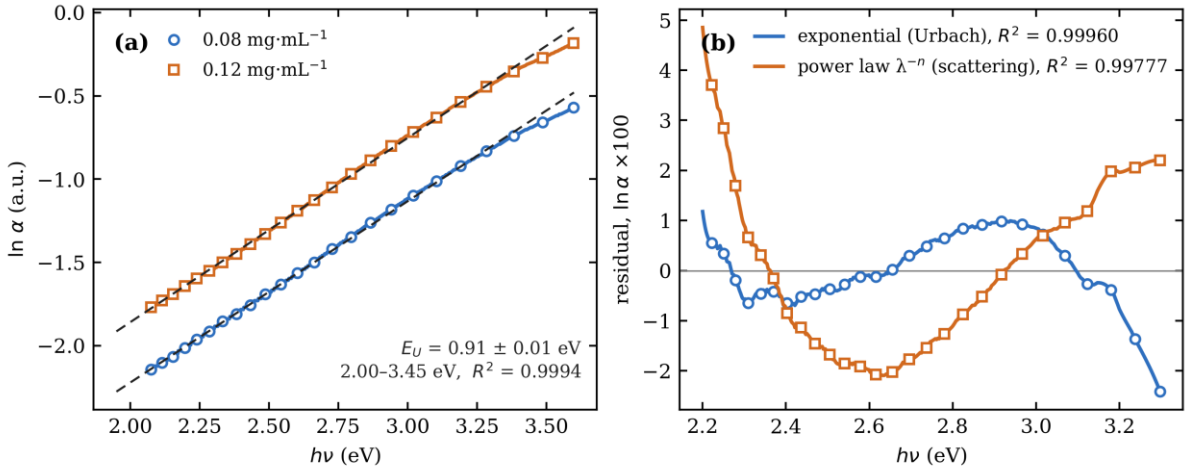


Figure 3. (a) Urbach plot and its linear approximation over the 2.00–3.45 eV range. (b) Residuals of the exponential (Urbach) and power-law λ^{-n} (scattering) models over 2.2–3.3 eV (0.12 mg·mL^{-1}, smoothed for display)

Because the measurement was performed on an aqueous dispersion, the observed tail could in principle have resulted from light scattering. To exclude this, two models were compared over the 2.2–3.3

eV range. the exponential model gave R^2 = 0.99960 and the power-law λ^{-n} model R^2 = 0.99777. The distribution of the residuals is even more indicative. for the power-law model the residuals have a systematic S shape and an amplitude two to three times larger than for the exponential model (Figure 3b). The observed tail is therefore not a scattering artefact but genuine band-tail absorption.

The value E_U = 0.91 eV is several times larger than the 10–100 meV typical of crystalline semiconductors. The steepness parameter $\sigma = kT/E_U$ equals 0.028 at 300 K and the ratio E_U/E_g equals 0.27. These values indicate a strongly smeared band edge, that is, a high fraction of sp^3 defects and small, isolated sp^2 domains. The conclusion is fully consistent with the Raman (I_D/I_G = 0.83, no 2D band observed) and EDS (C/O = 1.54) results reported in [9], as well as with data showing that the defect density increases with oxidation time [13].

5. Two independent estimates of the sp^2 domain size. According to the Robertson–O'Reilly cluster model, E_g = 3.36 eV corresponds to $N \approx 3$ fused aromatic rings, the equivalent diameter of such a cluster is 0.45 nm. The Ferrari–Robertson relation applied to the Raman data gives $L_a \approx 1.2$ nm. Both estimates are below 2 nm, which corresponds to the second stage of the Ferrari–Robertson amorphization trajectory and makes the use of the adopted C' coefficient self-consistent.

The factor of about 2.7 between the two estimates is not a contradiction but is physically expected. the optical estimate "sees" only the fully conjugated sp^2 cluster, whereas the Raman L_a gives the in-plane correlation length, which also includes distorted regions, so $L_a > d$ is natural. Tuinstra–Koenig type relations, by contrast, are not applicable in this case at all. depending on the coefficient adopted they give values in the 5–23 nm range, which contradicts the complete absence of the 2D band and shows that the range of validity of the model (L_a > 2 nm) has been exceeded [14].

Table 2. Summary of the optical parameters determined in this work

Parameter	Value	Condition / fitting window	R^2
π→π* maximum	230.5 nm	all three concentrations	—
ε_{230}	7.9 mL·mg^{-1}·cm^{-1}	Beer–Lambert, 3 points	0.9997
n→π* (2nd derivative)	304–305 nm	—	—
Eg (n = 2)	3.36 eV	3.70–4.15 eV	0.9992
Eg (n = 1/2)	1.87 eV	3.45–4.05 eV	0.9992
EU	0.91 ± 0.01 eV	2.00–3.45 eV	0.9994
EU (close to band edge)	0.96–0.98 eV	2.80–3.40 eV	0.999
σ = kT/EU (300 K)	0.028	—	—
EU/Eg	0.27	—	—
N (aromatic rings)	≈ 3	Robertson–O'Reilly	—
Cluster diameter	≈ 0.45 nm	Robertson–O'Reilly	—
La (Raman)	≈ 1.2 nm	Ferrari–Robertson	—

6. Application of the parameters obtained. The values determined here are directly required for the study of GO-based magneto-optical systems. In GO/Fe_3O_4 hybrid systems the magnetic circular dichroism (MCD) signal is proportional to the energy derivative of the absorption profile, while the Kerr rotation is linked to the absorption spectrum through the Kramers–Kronig relation. In a matrix with E_U = 0.91 eV the MCD lines belonging to the Fe^{3+}/Fe^{2+} transitions at the tetrahedral and octahedral sites of Fe_3O_4 are expected to overlap strongly, and a signal is expected to appear even below the band gap [15]. Re-measuring E_U in composite samples then allows two mechanisms to be distinguished. an increase in E_U indicates that the Fe_3O_4 particles have introduced additional structural disorder, whereas a red shift of the absorption edge at constant E_U indicates restoration of the sp^2 domains or GO ↔ Fe^{3+} charge transfer. The values obtained in this work serve as the zero point for that comparison.

Conclusions.

1. The Urbach energy of graphene oxide synthesized by the Hummers method was determined for the first time. E_U = 0.91 ± 0.01 eV, exponential region 2.00–3.45 eV, R^2 = 0.9994. The result is independent of concentration, and a model comparison showed that it is not a light-scattering artefact.

2. The position of the n→π* shoulder was estimated by three methods, and the systematic discrepancy between them was found to reach 20 nm (0.25 eV), although the reproducibility of each individual method is better than 2 nm. This accounts for a substantial part of the spread found in the literature and requires the method to be stated whenever the shoulder position is reported.

3. The Tauc analysis was shown to give the same quality of fit (R^2 = 0.9992) for both the n = 2 and the n = 1/2 model. Conclusions about the transition type must therefore not rest on the linearity of a Tauc plot alone.

4. The sp^2 domain size was estimated in two independent ways. 0.45 nm ($N \approx 3$ rings) from the optical data and 1.2 nm from the Raman data. Both values are below 2 nm, and the difference between them is explained by the physical meaning of the two methods.

5. The values E_g = 3.36 eV and E_U = 0.91 eV obtained here are proposed as baseline parameters for the interpretation of MCD and Kerr spectra in GO/Fe_3O_4 systems.

REFERENCES:

1. Donato K.Z., Tan H.L., Marangoni V.S., Martins M.V.S., Ng P.R., Costa M.C.F., Jain P., Lee S.J., Koon G.K.W., Donato R.K., Castro Neto A.H. Graphene oxide classification and standardization // Scientific Reports. — 2023. — Vol. 13. — 6064.

2. Krishnamoorthy K., Veerapandian M., Yun K., Kim S.-J. The chemical and structural analysis of graphene oxide with different degrees of oxidation // Carbon. — 2013. — Vol. 53. — P. 38–49.

3. Lai Q., Zhu S., Luo X., Zou M., Huang S. Ultraviolet-visible spectroscopy of graphene oxides // AIP Advances. — 2012. — Vol. 2. — 032146.

4. Aliyev E., Filiz V., Khan M.M., Lee Y.J., Abetz C., Abetz V. Structural characterization of graphene oxide. surface functional groups and fractionated oxidative debris // Nanomaterials. — 2019. — Vol. 9. — 1180.

5. Maphiri V.M., Bakhoum D.T., Sarr S., Sylla N.F., Rutavi G., Manyala N. Impact of thermally reducing temperature on graphene oxide thin films and microsupercapacitor performance // Nanomaterials. — 2022. — Vol. 12. — 2211.

6. Yu H., Zhang B., Bulin C., Li R., Xing R. High-efficient synthesis of graphene oxide based on improved Hummers method // Scientific Reports. — 2016. — Vol. 6. — 36143.

7. Dimiev A.M., Halbig C.E., Talyzin A. A critical review to avoid common misinterpretations in characterizing graphene oxide // Chemical Reviews. — 2026. — Vol. 126. — P. 3055–3088.

8. Urbach F. The long-wavelength edge of photographic sensitivity and of the electronic absorption of solids // Physical Review. — 1953. — Vol. 92. — P. 1324.

9. Daminov R., Ochilov O., Malikov K.Kh., Yoldoshev O., Qambarova M., Nematova Z., Turdiyev U. Cross-validated assessment of the oxidation degree of Hummers-derived graphene oxide by Raman, UV–Vis, and SEM–EDS // [journal]. — [year]. — [volume]. — [pages].

10. Tauc J., Grigorovici R., Vancu A. Optical properties and electronic structure of amorphous germanium // Physica Status Solidi B. — 1966. — Vol. 15. — P. 627–637.

11. Robertson J., O'Reilly E.P. Electronic and atomic structure of amorphous carbon // Physical Review B. — 1987. — Vol. 35. — P. 2946–2957.

12. Ferrari A.C., Robertson J. Interpretation of Raman spectra of disordered and amorphous carbon // Physical Review B. — 2000. — Vol. 61. — P. 14095–14107.

13. Saxena S., Kumar A., Yadav N., Jung S., Sharma M.K., Jeon S.-C., Koo B.H. Influence of oxidation time on defect density and crystallinity in graphene oxide synthesized via modified Hummer's method // Journal of Physical Chemistry Letters. — 2025. — Vol. 16. — P. 10932–10937.

14. Tuinstra F., Koenig J.L. Raman spectrum of graphite // Journal of Chemical Physics. — 1970. — Vol. 53. — P. 1126–1130.

15. Zubir N.A., Yacou C., Motuzas J., Zhang X., Diniz da Costa J.C. Structural and functional investigation of graphene oxide–Fe3O4 nanocomposites for the heterogeneous Fenton-like reaction // Scientific Reports. — 2014. — Vol. 4. — 4594.